

## Article

# Study on the Influence of the Joint Angle between Blast Holes on Explosion Crack Propagation and Stress Variation

Xiangyang Wang<sup>1,2</sup>, Xiantang Zhang<sup>1,2,\*</sup> , Jingshuang Zhang<sup>3</sup>, Hongmin Zhou<sup>1,2</sup>, Peng Zhang<sup>1,2</sup> and Dan Li<sup>1,2</sup>

<sup>1</sup> Shandong Provincial Key Laboratory of Civil Engineering Disaster Prevention and Mitigation, Shandong University of Science and Technology, Qingdao 266590, China; wxyhnl99@163.com (X.W.); skd992064@sdust.edu.cn (H.Z.); zhangpeng58305@163.com (P.Z.); ldxy1990@163.com (D.L.)

<sup>2</sup> College of Civil Engineering and Architecture, Shandong University of Science and Technology, Qingdao 266590, China

<sup>3</sup> Engineering Research Center of Underground Mine Construction, Ministry of Education, (Anhui University of Science and Technology), Huainan 232001, China; hnaust@163.com

\* Correspondence: zzxhtm@sdust.edu.cn; Tel.: +86-137-8987-0831

**Abstract:** The joints and fissures in a natural rock mass can affect the mechanical properties of the rock mass, the propagation of a blasting stress wave, and the blasting effect of the smooth surface of roadways. In the process of roadway drilling and blasting, there will inevitably be some joints between the two blast holes. Taking the joint angle as the starting point, this paper studies the rule of rock explosion crack propagation and stress variation when there are joints with different angles between two blast holes and analyzes the influence of joints on rock mechanical properties and blasting effects. The numerical simulation method and the software ANSYS/LS-DYNA are used to establish 7 rock mass models with various joint angles. When there is no joint between two holes and joints of 15°, 30°, 45°, 60°, 75°, and 90°, the propagation of explosive cracks and stress variations in the rock mass are discussed. The results show that the joints at different angles have obvious guiding and blocking effects on the propagation of explosive cracks, and as joint angles increase, the guiding effect becomes more apparent and the blocking effect becomes weaker. The effective stress of the rock mass will vary depending on the angles of the joints between the hole and the joint. As the joint angle increases, the joint's influence on the reflection and superposition of stress waves gradually weakens, and the peak value of the effective stress of the rock mass gradually decreases. The peak effective stress of the rock mass on the blasting side of the joint is similarly impacted by the superposition of stress waves, and the extreme value may be seen at the critical node of each change curve. The explosive crack will break through at the critical location because the maximal effective stress of the rock mass is distributed in a "W" form on the blasting side of the joint.

**Keywords:** joint angle; crack propagation; effective stress; stress wave; numerical simulation



**Citation:** Wang, X.; Zhang, X.; Zhang, J.; Zhou, H.; Zhang, P.; Li, D. Study on the Influence of the Joint Angle between Blast Holes on Explosion Crack Propagation and Stress Variation. *Processes* **2023**, *11*, 2805. <https://doi.org/10.3390/pr11092805>

Academic Editors: Qingbang Meng, Chun Feng, Chenxi Ding, Jianguo Wang, Chun Liu and Liyun Yang

Received: 13 August 2023

Revised: 11 September 2023

Accepted: 18 September 2023

Published: 21 September 2023



**Copyright:** © 2023 by the authors. Licensee MDPI, Basel, Switzerland. This article is an open access article distributed under the terms and conditions of the Creative Commons Attribution (CC BY) license (<https://creativecommons.org/licenses/by/4.0/>).

## 1. Introduction

Due to the influence of geological structure and surface external force, various discontinuous structural planes are formed in natural rock masses, such as joint cracks, bedding, weathered interlayers, and pelletized interlayers. Among them, joint cracks are the most widely distributed structural plane in rock masses [1]. The existence of joints in a rock mass seriously affects the mechanical properties of the rock mass, the smooth blasting forming effect, and the stability of the surrounding rock after blasting, among which the joint angle has the greatest influence on the smooth blasting forming effect of roadways [2,3]. Therefore, this paper takes the joint angle as the starting point to study the expansion of explosive cracks in rock masses under different joint angles and the stress variation of rock mass elements, and it summarizes the specific influence of different joint angles on the smooth blasting of roadways to provide guidance for practical engineering.

The procedure and results of a rock's cracking may be seen directly based on the explosive crack's propagation. As a result, several studies on the explosive crack propagation mechanism of jointed rock masses have been conducted both nationally and internationally. Ding et al. [4] used the dynamic caustic test system to study the interaction between the directional crack of the slit charge and the open joint and found that the open joint blocked the expansion of the directional crack and that two wing cracks would occur at the end of the open joint. In order to study the crack propagation rules of unfilled joints under blasting, Xu, Li, and Yang et al. [5–7] used the dynamic caustic test system and the numerical simulation software ABAQUS. They discovered that the inclined joint end produced an obvious stress concentration under the action of shock wave diffraction, making the joint end more susceptible to the initiation of wing cracks. Zhang et al. [8] used LS-DYNA software to numerically simulate the blasting process of jointed rocks with different joint lengths, positions, and filling media under static stress and described the propagation rules of explosive cracks under various joint conditions. Through model tests, Liang et al. [9] studied the crack propagation process of cross-fractured rock masses with different inclination angles under impact loads and found that the inclination angle of the main fracture would affect crack initiation and polymerization. Wei et al. [10] used numerical simulation to study the propagation rules of explosive cracks with various ground stresses and joint angles and found that explosive cracks were more likely to expand along the inclined direction of joints.

When the rock mass contains joints, the propagation of the explosion stress wave in the rock mass is influenced, as is the change in the effective stress and crack propagation of the rock mass. As a result, scientists both at home and abroad have done extensive studies on the propagation of explosion stress waves in jointed rock masses. Fan and Song et al. [11,12] studied the attenuation rules of explosive stress waves in single-jointed rock masses by combining numerical simulation and field tests and found that with an increase in the joint inclination angle, the attenuation of explosive stress waves increased and the amplitude of stress waves decreased. Li et al. [13] studied the effect of different joint numbers on the attenuation of explosive stress waves through model tests and deduced the propagation equation of stress waves at multiple nonlinear joints. Sun [14] used ANSYS/LS-DYNA software to study the influence of different sandwich properties on the propagation rules of explosive stress waves and concluded that the smaller the angle between the weak sandwich and the horizontal measurement line, the stronger the barrier effect on stress waves. Qu et al. [15] combined theoretical analysis, numerical simulation, and an indoor model test to study the attenuation of explosion stress waves in rock masses under different joint angles, and the results showed that the attenuation of explosion stress waves accelerated with the increase of joint angles. Liu et al. [16] used DIC technology, studied the influence of different crack inclination angles on the distribution of the stress-strain field in shale specimens, analyzed the law of crack initiation, propagation, and destruction in shale specimens from the perspective of stress, and found that the evolution of the stress-strain field would have an impact on crack initiation and propagation.

To summarize, there have been many studies on the effects of explosive crack propagation and explosion stress wave propagation in jointed rock masses, but there are still the following deficiencies that need to be further studied: in terms of the number of holes, current studies mainly focus on single-hole blasting and do not consider the effects of the joint between the blast holes on stress wave propagation and crack propagation in the simultaneous initiation of dual holes. In terms of joint types, the current research mainly focuses on unfilled joints, and there are few studies on joints with rock, soil, and gravel filling. In the study of stress waves, the effect of stress wave propagation on the effective stress of rock masses is not considered. Therefore, this paper innovates in terms of the number of holes and joints and studies the influence of filling joints at different angles between two holes on crack propagation and mechanical properties of rock masses, hoping that the research results can play a certain guiding role in engineering practice.

## 2. Joint Angle's Influence on Rock Element Stress

In the following content, the influence of parameters like joint thickness is not taken into account in order to simplify the problem and focus just on one variable of joint angle. This paper's numerical model is simplified in Figure 1a.  $\alpha$  is the angle between the connection of the blast hole and the direction of the normal line of the joint,  $\beta$  is the angle between the connection between any point on the joint and the center of the blast hole and the direction of the normal line of the joint, and  $\theta$  is the angle between any point on the joint and the line between the center of the blast hole. A finite element is taken at point D, and its stress variation rule is studied. Point C is the midpoint of the connection between the two holes, and point E is the vertical foot of the hole and the joint. Figure 1b illustrates its stressed state.

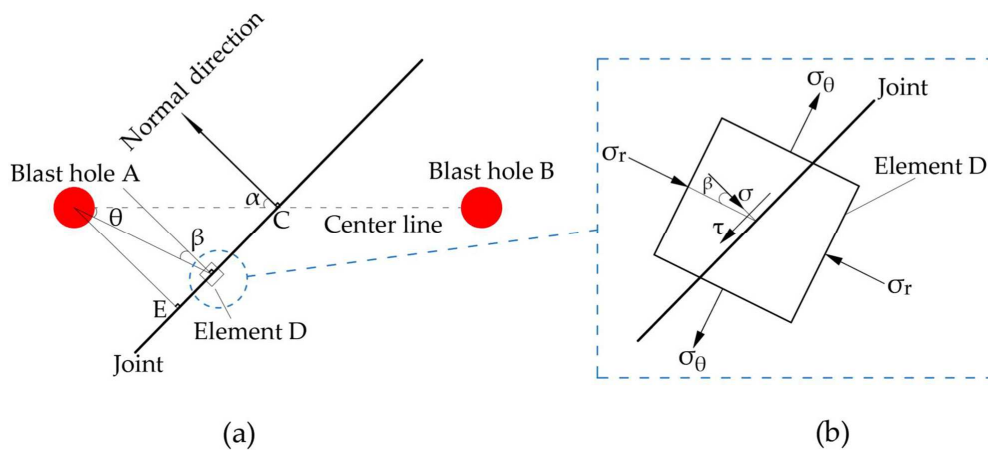


**Figure 1.** Stress analysis diagram. (a) Schematic diagram of theoretical analysis model; (b) Stressed state of element D.

The Moore–Coulomb strength hypothesis [1] states that the element's normal stress and shear stress at point D are as follows:

$$\begin{cases} \sigma = \frac{\sigma_r + \sigma_\theta}{2} + \frac{\sigma_r - \sigma_\theta}{2} \cos 2\beta \\ \tau = \frac{\sigma_r - \sigma_\theta}{2} \sin 2\beta \end{cases} \quad (1)$$

where  $\sigma$  is the normal stress of the element at point D;  $\tau$  is the shear stress of the element at point D;  $\sigma_\theta$  is the annular tensile stress;  $\sigma_r$  is radial compressive stress; and  $\beta$  is the angle between the radial compressive stress and the normal stress of the element.

According to the study on the strength theory of single structural plane rock mass [15,17], the relationship between the toroidal tensile stress and radial compressive stress of the element at point D is as follows:

$$\sigma_\theta = -b\sigma_r \quad (2)$$

where  $b = \nu/(1 - \nu)$ ,  $\nu$  is Poisson's ratio.

As a result, the element's shear stress and normal stress at point D are stated as follows:

$$\begin{cases} \sigma = \frac{\sigma_r}{2} [(1 - b) + (1 + b) \cos 2\beta] \\ \tau = \frac{\sigma_r}{2} (1 + b) \sin 2\beta \end{cases} \quad (3)$$

In accordance with the conventions of rock mechanics concerning symbols, the tensile force is specified as positive and the pressure as negative. Then, the radial compressive stress is  $\sigma_r < 0$  and the circumferential tensile stress is  $\sigma_\theta > 0$ . Assuming that the normal stress of the element at point D in Figure 1b is compressive stress, that is,  $\sigma_r \leq 0$ , it can be deduced from Formula (3) that:

$$(1 - b) + (1 + b) \cos 2\beta \geq 0 \quad (4)$$

In other words, the element D is stressed in the following range:

$$-\frac{1}{2} \cos^{-1} \left( \frac{b-1}{b+1} \right) \leq \beta \leq \frac{1}{2} \cos^{-1} \left( \frac{b-1}{b+1} \right) \quad (5)$$

When  $\beta$  no longer satisfies the range of Equation (5), the above assumption is not valid. That is, the stress at  $\sigma > 0$ , D becomes tensile stress, and when the tensile stress of the rock mass is greater than the dynamic tensile strength of the rock, the rock will be damaged.

According to the geometric relationship shown in Figure 1a:

$$\beta = \alpha - \theta \quad (6)$$

As a result, the current value range of  $\alpha$  is:

$$\theta - \frac{1}{2} \cos^{-1} \left( \frac{b-1}{b+1} \right) \leq \alpha \leq \theta + \frac{1}{2} \cos^{-1} \left( \frac{b-1}{b+1} \right) \quad (7)$$

By simplifying Equation (7), it can be concluded that, when  $0 < \alpha < \frac{1}{2} \cos^{-1} \left( \frac{b-1}{b+1} \right)$ , the stress is maximized in the direction of the vertical connection between the blast hole and the joint. With the movement of the measuring point element, the angle gradually increases, and the stress on both sides decreases. When  $\frac{1}{2} \cos^{-1} \left( \frac{b-1}{b+1} \right) < \alpha < 90^\circ$ ,  $\sigma > 0$ , the normal stress of the element is tensile stress, the existence of the joint blocks the propagation of stress waves, and it affects the rock breaking effect of the rock mass behind the joint structural plane.

Through the above analysis, the general rules of stress variation of a rock mass on the blasting side of the joint were obtained. With the change of joint angle and joint properties, the rules will change correspondingly. Subsequently, the stress variation rules of different models in this paper will be analyzed according to the theoretical analysis in this section. For detailed analysis, see Section 5.2.

### 3. Calculation Model and Material Parameters

#### 3.1. Calculation Model

In order to study the effect of different joint angles on blasting effects, seven different calculation models are established using ANSYS/LS-DYNA software. The calculation model in this research is established as a planar strain model [18] to simplify calculation and save calculation time, and the calculation model is presented in Figure 2.

The time-domain half-plane boundary element method (BEM) [19,20] is the main method to solve the boundary elastic dynamics problem in the semi-infinite region, which can effectively improve calculation accuracy and save calculation time compared with the full-plane BEM. However, the model in this paper is limited in size and does not want to consider the reflection effect of boundary conditions on stress waves, so the boundary conditions in this paper are all non-reflecting boundaries, and the time-domain half-plane boundary element method (BEM) is not applicable.

The propagation speed of stress waves in a rock mass and the size of the numerical model are comprehensively considered to ensure that there is no interference from boundary-reflected stress waves in the process of rock breaking by blasting and that the explosion stress waves have a full effect on the rock mass [21–26]. In this paper, the size of the calculation model is designed to be 5 m × 5 m × 0.01 m, and non-reflecting boundaries are set around the model [21]. According to the provisions of “Blasting Safety Regulations” and combined with the actual situation of the model, the following is set: the spacing of two holes is 0.6 m, the radius of the hole is 0.016 m, the depth of the hole is 0.01 m, the charge structure is coupled, and the radius of the cartridge is 0.016 m. The joint length is 1.0 m, the width is 0.002 m, and the distance between the joint center and the hole center is 0.3 m. The angle between the center line of the blast hole and the center line of the joint is the joint inclination angle, which can be no joint, 15°, 30°, 45°, 60°, 75°, or 90°.

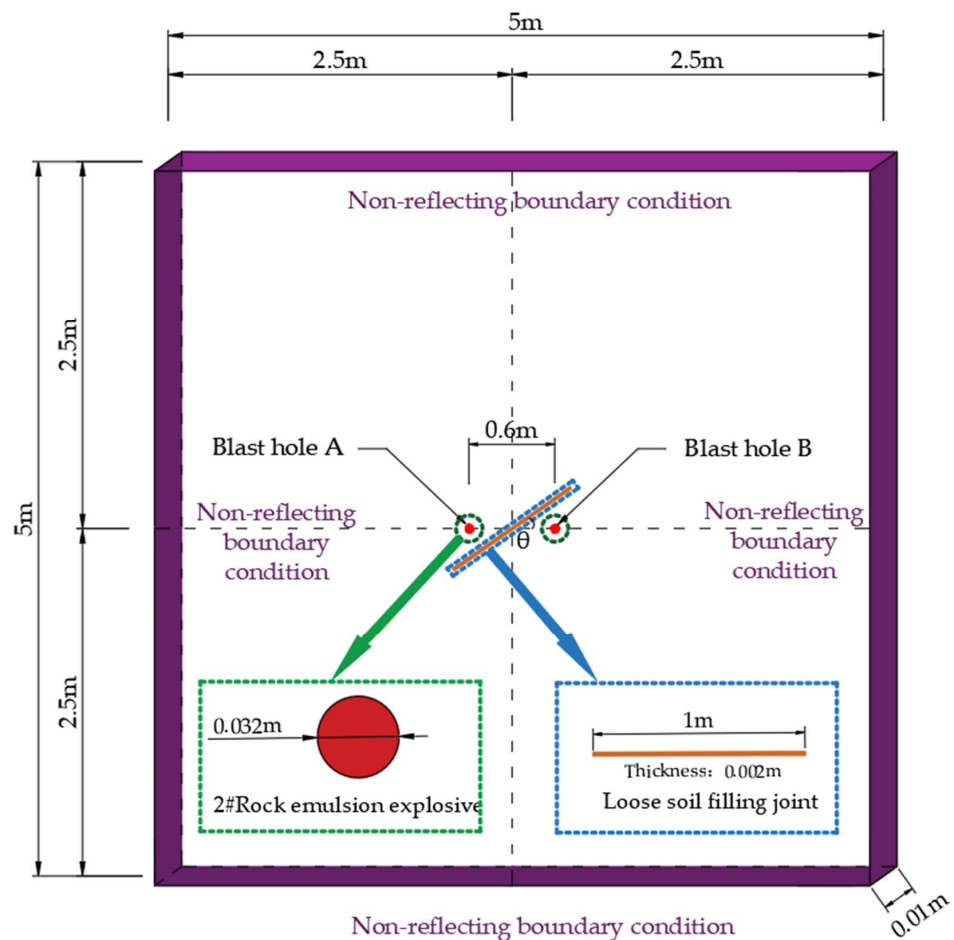


Figure 2. Schematic diagram of calculation model.

The angle of the joint is inconsistent among the models in this paper, and the difference of the grid division between the different models will cause a little calculation error. Therefore, this paper adopts the method of reducing the irregular grid area and refining the whole finite element mesh to reduce the calculation error. The whole grid is divided by using the “VMESH” method, the irregular area is divided by using the “VSWEEP” method, and the mesh size is controlled to 5 mm (except for irregular mesh).

All elements in the model are Solid164 solid elements; the ALE algorithm is used to calculate explosives and air elements; and the Lagrange algorithm is used to calculate rock and joint elements. The explosives are all centrally initiated, and the calculated termination time is 0.0006 s.

### 3.2. Material Parameters

In this paper, granite is selected as the rock material, and the RHT material model is used to describe the failure process and damage characteristics of rock. The rock material parameters are defined by the keyword \*MAT\_RHT, and related material parameters are shown in Table 1 [22,23]. The joint filling material is made of loose soil, and the keyword \*MAT\_PLASTIC\_KINEMATIC is used to define the joint filling material. The specific material parameters are shown in Table 1 [24].

The 2# rock emulsion explosive was selected for the explosive. The JWL equation of state was used to reflect the relationship between the volume and pressure of detonation products after explosion. The explosive material parameters are defined with the keyword

\*MAT\_HIGH\_EXPLOSIVE\_BURN, and the equation of state parameters are defined with the keyword \*EOS\_JWL. The equation of state for the explosives is as follows:

$$P = A \left( 1 - \frac{\omega}{R_1 V} \right) e^{-R_1 V} + B \left( 1 - \frac{\omega}{R_2 V} \right) e^{-R_2 V} + \frac{\omega E_0}{V} \quad (8)$$

where  $P$  is the detonation pressure, MPa;  $V$  is the volume of detonation product,  $m^3$ ; and  $E_0$  is the initial specific internal energy of the detonation products.  $A$ ,  $B$ ,  $R_1$ ,  $R_2$ , and  $\omega$  are all material parameters, and the values of the related material parameters are shown in Table 2 [25].

The air material model is defined by the keyword \*MAT\_NULL, and the density of air is  $1.29 \text{ kg/m}^3$ . The equation of state of the air is defined by the keyword \*EOS\_LINEAR\_POLYNOMIAL, and the equation of state is:

$$P = C_0 + C_1 \mu + C_2 \mu^2 + C_3 \mu^3 + (C_4 + C_5 \mu + C_6 \mu^2) E \quad (9)$$

where  $C_0$ ,  $C_1$ ,  $C_2$ ,  $C_3$ ,  $C_4$ ,  $C_5$ , and  $C_6$  are the coefficients of the equation of state;  $E$  is the element initial internal energy of the relative volume; and  $\mu = 1/V - 1$ ;  $V$  is the relative volume of air. Among them, the values of  $C_4$  and  $C_5$  are both 0.4,  $E$  is 0.025 GPa, and the coefficients of other equations of state are 0 [24,26].

**Table 1.** Parameters of rock and joint filling materials.

| Materials  | Density/kg/m <sup>3</sup> | Elasticity Modulus/GPa | Yield Strength/MPa | Poisson Ratio | Compressive Strength/MPa |
|------------|---------------------------|------------------------|--------------------|---------------|--------------------------|
| Rock       | 2760                      | 55                     | 59.5               | 0.38          | 119                      |
| Loose soil | 1600                      | 14                     | 48                 | 0.27          | 78                       |

**Table 2.** 2# rock emulsion explosive materials and state equation parameters.

| Density kg/m <sup>3</sup> | Detonation Velocity/m/s | C-J Pressure/GPa | State Equation Parameter |       |                |                |          |                     |
|---------------------------|-------------------------|------------------|--------------------------|-------|----------------|----------------|----------|---------------------|
|                           |                         |                  | A/GPa                    | B/GPa | R <sub>1</sub> | R <sub>2</sub> | $\omega$ | E <sub>0</sub> /GPa |
| 1100                      | 3800                    | 10.5             | 374                      | 3.23  | 4.15           | 0.95           | 0.3      | 7                   |

### 3.3. Model Verification

Three calculation models were re-established in this section to ensure that the size and material parameters of the model mentioned above were reasonable. The overall size of the models was  $5 \text{ m} \times 5 \text{ m} \times 0.01 \text{ m}$ , and the material parameters, hole diameter, hole spacing, and hole and joint spacing were all consistent with those discussed in the first two sections.

The single hole blasting model was solved and compared with the granite test block experiment of Banadaki [23] et al., it was found that the experimental results were highly consistent with the simulation results, and the rock mass after the explosion all contained the crushing zone, fracture zone, and elastic vibration zone, indicating that the material model selected in this paper was reasonable (Figure 3a,d).

The single joint blasting model was solved and compared with the single prefabricated crack experiment of the PMMA plate conducted by Wang [27] et al., and it was found that the experimental results were highly consistent with the simulation results. The crack growth pattern of the rock mass after the explosion was basically the same, and wing cracks appeared at the joint ends, indicating that the joint parameters selected in this paper were reasonable (Figure 3b,e).

The two hole blasting model was solved and compared with the two hole blasting experiment of the PMMA plate by Cho [28] et al., it was found that the experimental results were highly consistent with the simulation results, the crack growth pattern of the rock mass after the explosion was basically the same, and the cracks were connected between

the two blast holes, indicating that the spacing of the gun holes selected in this paper was reasonable (Figure 3c,f).

To summarize, the model size, material parameters, and joint characteristics selected in this paper are practical, the subsequent simulation can accurately reflect the blasting process of rock, and the simulation results are real and reliable.

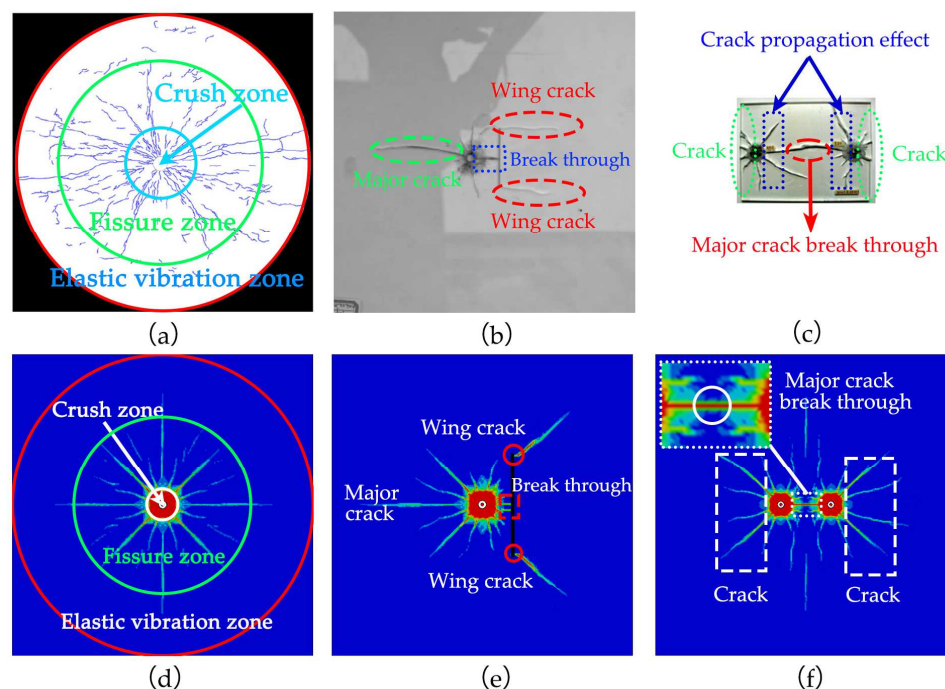


**Figure 3.** Comparison between simulation results and test results. (a) Experiment results of single hole [23]; (b) Experiment results of single joint [28]; (c) Experiment results of double hole [29]; (d) Simulation results of single joint; (e) Simulation results of single joint; (f) Simulation results of double hole.

#### 4. The Propagation Process of Explosive Cracks

In this paper, the influence of existing joints on the crack propagation time of a rock mass is studied, the phenomenon of crack propagation is controlled uniformly, and the variation rule of crack propagation time is observed. After the calculation was completed, damage cloud images at four typical moments of each model (visible damage can be regarded as a crack) were selected to study the crack propagation process [29]. The damage cloud images under different working conditions are shown in Figures 4–6.

As can be seen from Figure 4, at first a circular crushing zone was formed near the blast holes, and only the crushing zone caused damage in the non-jointed model, while damage occurred on the blasting side in the jointed model due to the reflection of stress waves (Figure 4a,e). With the propagation of stress waves, the stress waves of the left and right holes meet and superpose at the midpoint, and the damage between the two holes begins to extend. Due to the reflection and stretching action of stress waves at the joint, the superposition effect of stress waves between the blast holes is strengthened, so the penetrating time of damage between the two blast holes in the model with the joint is shorter (Figure 4b,f). With the gradual attenuation of the explosion stress wave, its final strength is not enough to make the crack continue to expand, and the explosive gas starts to push the crack to continue to expand [10]. The explosion hole's surrounding major cracks and micro-cracks began growing due to the explosive gas (Figure 4c,g). Finally, the cracks on the connection of the two blast holes in the non-jointed model were completely gone. The cracks in the jointed model no longer extended rearward once they reached the joint

because the joint's energy release allowed the explosive gas to escape. This indicates that the joint's presence will prevent the explosive cracks from spreading further (Figure 4d,h).

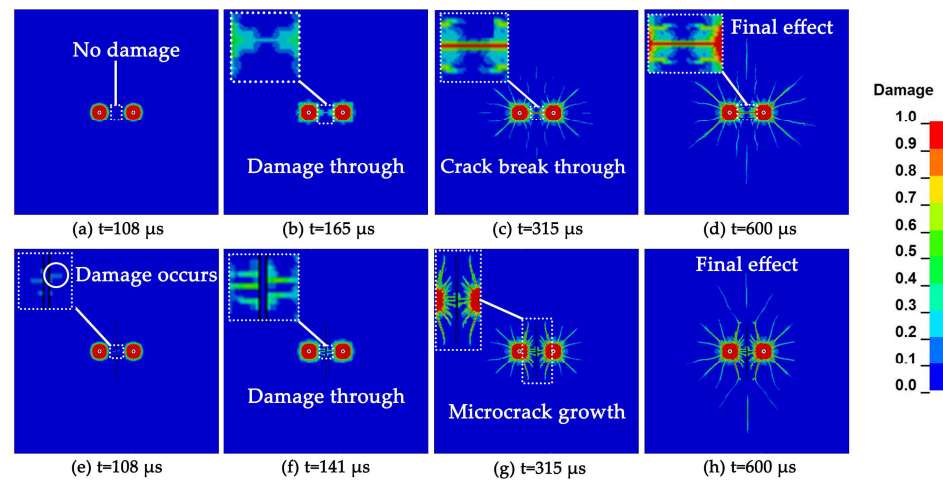


**Figure 4.** Damage cloud diagram at different joint angles. (a–d) no joints ( $\theta = 0^\circ$ ); (e–h)  $\theta = 90^\circ$ .

Figure 5 indicates that when the joint angle increases between  $15^\circ$  and  $30^\circ$ , the attenuation of stress waves increases, and the duration of reflected tensile damage on the side of the joint facing the explosion also increases (Figure 5a,e). As the stress wave propagates, it diffracts at the joint end, producing stress concentration and damage there, and the wing crack at the joint end begins to break through (Figure 5b,f). As a result of the explosive gas wedge's activity, the wing cracks expand along the inclined direction of the joint. When the stress waves created by the two holes are stacked, a stress concentration zone forms at the stress wave junction, deflecting the direction of microcrack formation (Figure 5c,g). Finally, all of the cracks expand in the previously mentioned path, with evident explosive cracks forming on the joint extension line, perpendicular to the joint direction, and in the stress concentration zone (Figure 5d,h).

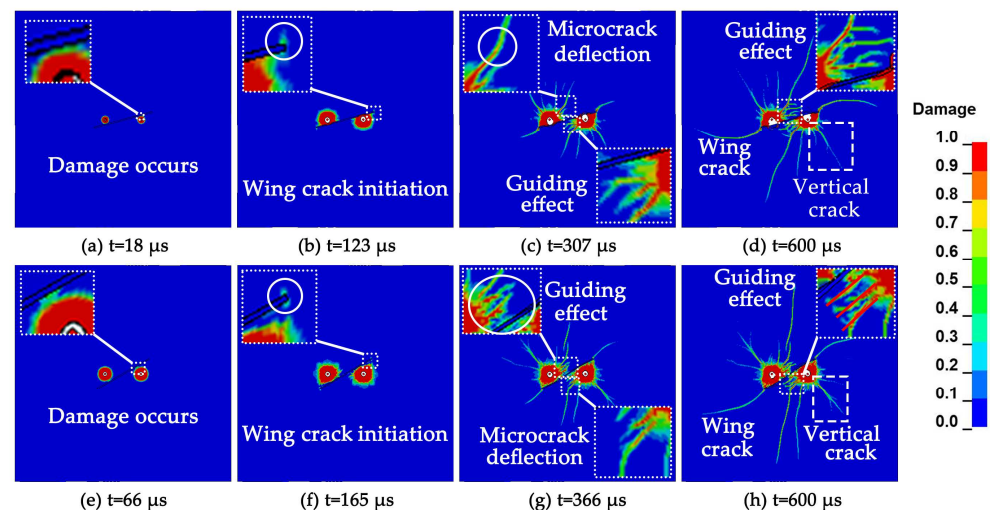


**Figure 5.** Damage cloud diagram at different joint angles. (a–d)  $\theta = 15^\circ$ ; (e–h)  $\theta = 30^\circ$ .

Figure 6 indicates that with the increase in joint angle, the damage occurs over a longer period of time. (Figure 6a,e,i). The explosion stress wave and the reflected tensile stress wave superimposed on each other in the direction vertical to the joint, inducing the microcracks through in this direction, and other microcracks propagated between the blast hole and the joint along the parallel direction. At the same time, with the increase in joint angle, the attenuation of the stress wave increased. Although there was stress concentration

at the end of the joint, it could no longer expand into wing cracks (Figure 6b,f,j). Subsequently, the explosion crack was also deflected under the superposition of stress waves (Figure 6c,g,k). Finally, all of the above cracks expanded along the original direction, and only some microcracks were generated. However, due to the blocking effects of the joint, only damage occurred in the rock mass on the back of the joint's explosion side, and no forming cracks occurred (Figure 6d,h,l).

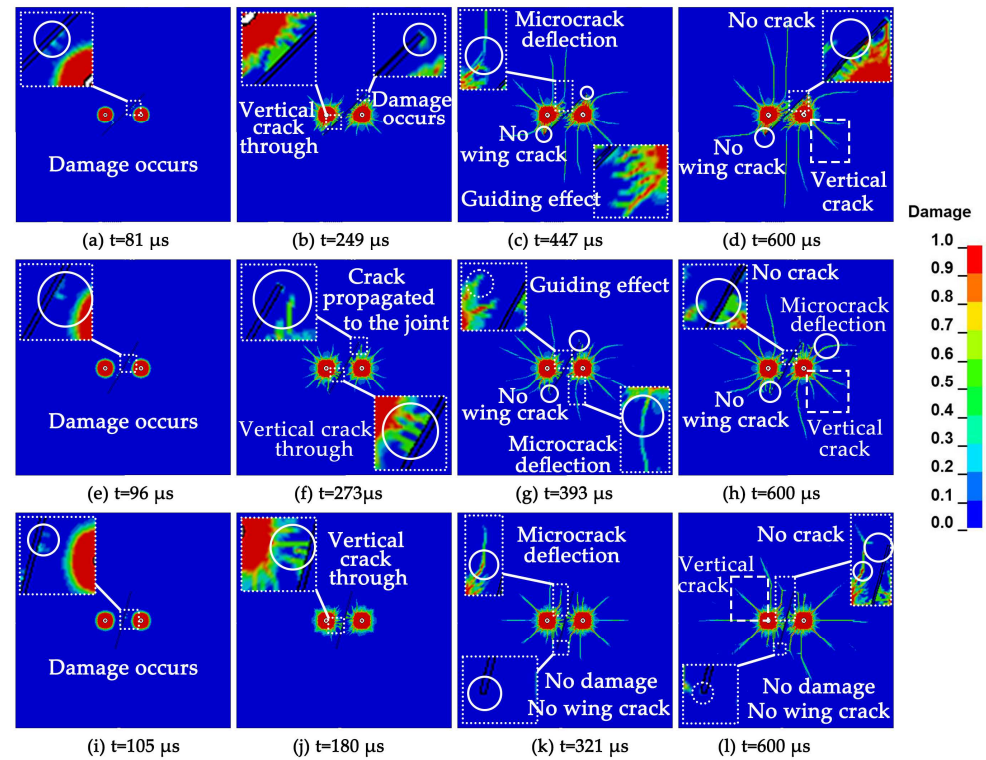


**Figure 6.** Damage cloud images at different joint angles ( $45^\circ$ ,  $60^\circ$ ,  $75^\circ$ ). (a–d)  $\theta = 45^\circ$ ; (e–h)  $\theta = 60^\circ$ ; (i–l)  $\theta = 75^\circ$ .

To summarize, joints at different angles have obvious guiding and blocking effects on the expansion of explosive cracks. With the increase in the joint angle, the time of damage on the blasting side of the joint increases, the time of crack penetration between the blast hole and the joint increases, the stress concentration effect of the joint end is weakened, and the wing crack no longer occurs in the joint end after  $45^\circ$ .

## 5. Rock Mass's Effective Stress

Under the impact of explosive stress waves, rocks are often brittle. Therefore, the criterion of rock damage fracture under the impact of explosive stress waves can be applied to the criterion of pure brittle damage fracture. Starting from the concept of equivalent stress, Lemaitre [30] claims that when the equivalent stress  $\sigma_e$  reaches the ultimate stress  $\sigma_u$  of the material, the damage reaches the critical value and the material breaks; that is, the one-dimensional damage fracture criterion:

$$\sigma_e = \sigma_u \quad (10)$$

$$\sigma_u = \sigma_{td} \quad (11)$$

where  $\sigma_e$  is the Mises effective stress,  $\sigma_u$  is the ultimate stress of the material, and  $\sigma_{td}$  is the dynamic tensile strength of the rock, which is 59.5 MPa in this paper. (Note: The Mises effective stress mentioned above is the same concept as the effective stress described below.)

Since the model in this paper is a plane strain model, only the one-dimensional damage fracture criterion is considered [30]. In other words, when the effective stress of the rock measuring point element is greater than the dynamic tensile strength of the rock, the element will have tensile fracture failure, and the crack will expand to that place. Therefore, in this paper, a number of measuring point elements at different positions are selected to study the change of the effective stress peak, and the crack propagation at key locations is analyzed from the stress angle.

5.1. Effective Stress of Rock Mass on the Connection of Two Blast Holes

The effective stress of the rock element on the connection of two holes under various joint angles is investigated in order to better investigate the cause of crack propagation between two holes. Due to the model’s symmetry, only six measuring point elements with  $d = 0.05$  m separation between hole A and the joint were chosen (Figure 7). Their effective stress peaks were read using LS-prepost software, and a graph of them is displayed in Figure 8.

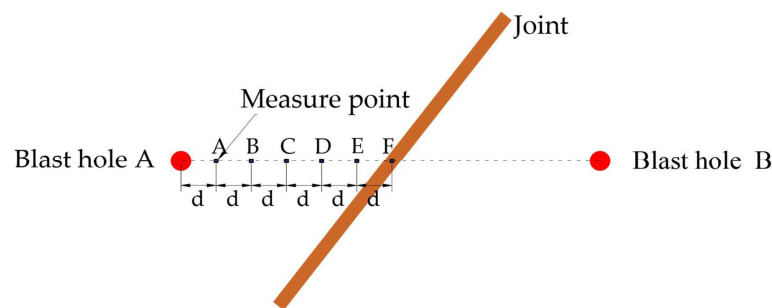


Figure 7. Layout of measuring point elements. ( center line of the two holes).

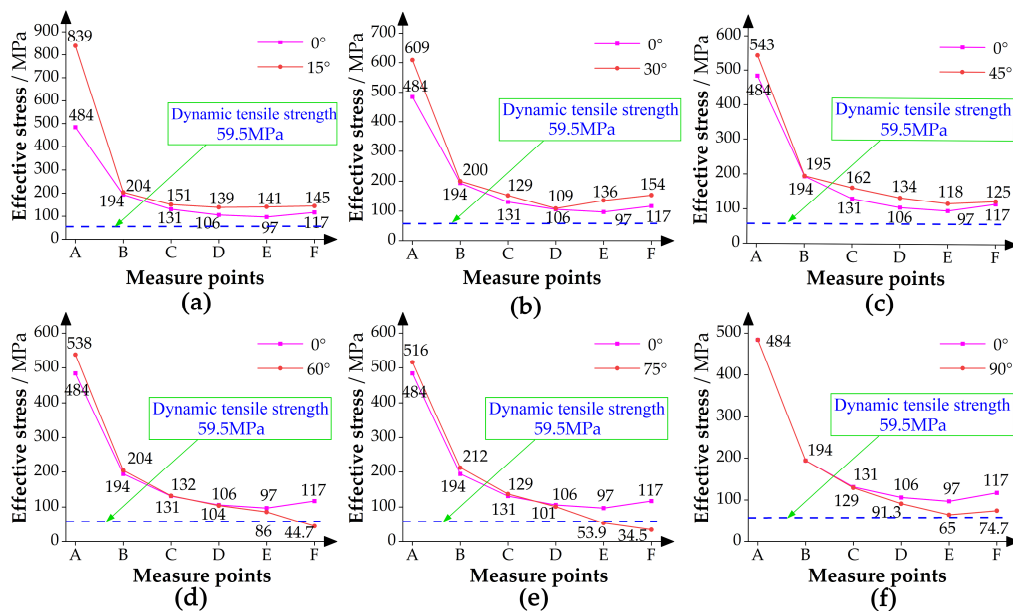


Figure 8. Variation diagram of peak effective stress. (a)  $\theta = 0^\circ$  and  $\theta = 15^\circ$ ; (b)  $\theta = 0^\circ$  and  $\theta = 30^\circ$ ; (c)  $\theta = 0^\circ$  and  $\theta = 45^\circ$ ; (d)  $\theta = 0^\circ$  and  $\theta = 60^\circ$ ; (e)  $\theta = 0^\circ$  and  $\theta = 75^\circ$ ; (f)  $\theta = 0^\circ$  and  $\theta = 90^\circ$ .

Figure 8 demonstrates that, without the existence of a joint between the two blast holes, the peak value of effective stress at measuring points A to E gradually decreases, indicating that the explosion stress wave will weaken as it travels through the rock, while the peak value of the effective stress at measuring point F rises as a result of the superposition of stress waves. When there is a  $90^\circ$  joint between the two holes, the peak value of the

effective stress at the measuring point C~F is significantly lower than that without the joint. This indicates that the joint has a blocking effect on the stress wave propagation, so the effective stress peak value decreases (Figure 8f). Meanwhile, the peak effective stress of all measuring points is much greater than the dynamic tensile strength of the rock, so the rock mass elements in the middle of the two holes have been destroyed, and the main explosive cracks on the line of the hole have been penetrated.

When there is a joint between the two holes and the joint angle is small, the variation trend of the peak effective stress of the measuring point element is the same as that without a joint. However, due to the presence of joints, stress waves are reflected and transmitted, the stress field between the hole and the joint is strengthened, and the peak value of the effective stress at all measuring points is greater than that without a joint (Figure 8a–c). Therefore, the main explosive cracks on the central line of the two holes have been penetrated.

As the joint angle grows, so does the vertical distance between the measurement point element and the joint, as well as the propagation distance of the reflected stress wave. As a result, the peak value of the effective stress at measuring locations D~F drops gradually and is less than the peak value of the effective stress without joints (Figure 8d,e). Meanwhile, there are portions in both figures whose peak effective stress is less than the dynamic tensile strength of the rock, indicating that the fractures between the two blast holes are not completely penetrated when the joint inclination is  $60^\circ$  and  $75^\circ$ .

To summarize, the presence of joints affects the reflection and superposition of stress waves between the hole and the junction, which in turn affects the effective stress of the rock mass. When the joint angle is small ( $15\sim 45^\circ$ ), the reflection and superposition of stress waves are enhanced, the peak effective stress of the rock element between the blast hole and the joint is increased (when compared to that without the joint), the cracks on the blast hole line are connected, and the rock breaking effect is improved. When the joint angle is large ( $60\sim 90^\circ$ ), the superposition of stress waves near the joint is weakened, and the peak value of the effective stress near the joint is gradually reduced.

### 5.2. Effective Stress of Rock Mass on Blasting Side

In this section, the effective stress of the rock element on the blasting side at various angles is examined in order to further investigate the crack propagation between the hole and the blasting side of the joint. Because of the central symmetry of the model, only 11 measuring points were selected at equal spacing on the blasting side of the joint corresponding to hole A, with spacing  $d = 0.05$  m (as shown in Figure 9). Their effective stress peaks were read using LS-prepost software, and a graph of them is depicted in Figure 10.

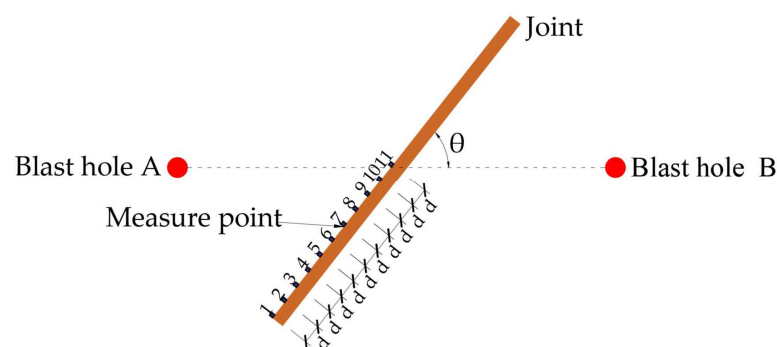


**Figure 9.** Layout of measuring point elements.

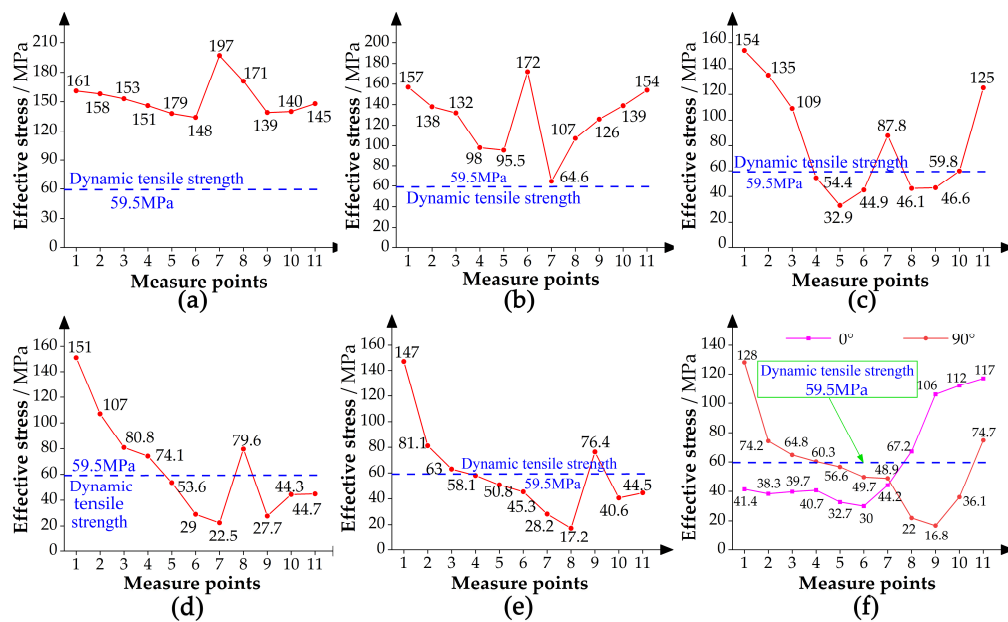


**Figure 10.** Variation diagram of peak effective stress. (a)  $\theta = 15^\circ$ ; (b)  $\theta = 30^\circ$ ; (c)  $\theta = 45^\circ$ ; (d)  $\theta = 60^\circ$ ; (e)  $\theta = 75^\circ$ ; (f)  $\theta = 0^\circ$  and  $\theta = 90^\circ$ .

As shown in Figure 10, there are three extreme value points (except  $90^\circ$ ) on each curve, which makes the graph appear as a “W” shape. The measuring point elements corresponding to the three extreme value points are rock mass elements at the joint end, rock mass elements perpendicular to the blast hole, and rock mass elements at the midpoint of the blast hole connection, respectively. The diagram depicts a “V” form when the joint inclination is  $90^\circ$  because there are only two extreme value points, and the rock mass element perpendicular to the blast hole is at the center of the blast hole connection.

It is found that when there is a joint between hole A and hole B, the superposition position of the stress wave changes, the stress concentration occurs at the joint end, and the peak value of the effective stress of the rock element at the joint end increases. When the distance between the measuring point element and the joint is the shortest, the amplitude attenuation of the stress wave is the smallest, the peak effective stress of the rock mass element increases significantly, and the effective stress of the elements on the left and right sides of the element decreases gradually [15]. The rock element at the middle point of the blast hole line increases slightly due to the superposition of the left and right stress waves.

When the joint angle is small, the peak effective stress of all measuring points is greater than the dynamic tensile strength of the rock, indicating that at this time, the rock mass on the blasting side of the joint has been destroyed, the cracks between the blast hole and the joints have penetrated all the way through (Figure 10a,b), and the rock crushing effect is good. When the joint angle is large, only the joint end, the shortest distance, and the crack on the blast hole line are connected (Figure 10c–f), and the rock crushing effect is poor, which may increase the bulk rate.

In conclusion, the blasting effect worsens as the joint angle increases, changing the superposition position of stress waves and the stress concentration effect at the joint end and gradually weakening the effective stress peaks at the three extreme locations.

## 6. Conclusions

There are many joints and fissures in natural rock, and there are some problems such as poor blasting forming effect and poor stability of surrounding rock in the process of blasting excavation, which seriously affect the blasting excavation efficiency and safety of construction personnel. In this paper, the problem is simplified and analyzed simply by using a numerical simulation method. The influence of different joint angles between

blast holes on the blasting effect of rock mass is studied. Seven different blasting models from different angles are established and solved by using ANSYS/LS-DYNA software. The conclusions are as follows:

1. Joints at different angles have obvious guiding and blocking effects on the growth of explosive cracks. The explosive crack near the joint will expand along the direction parallel to the joint. The wing crack at the end of the joint expands along the inclined direction of the joint. With the increase of the joint angle, the time of the crack penetrating between the hole and the joint increases, and the stress concentration at the joint end is weakened.
2. The existence of the joint will affect the reflection and superposition of stress waves and then affect the effective stress of the rock mass. When the joint angle is between  $15^\circ$  and  $45^\circ$ , the reflection and superposition of stress wave are strengthened, and the peak effective stress of the rock along the central line decreases first and then increases slightly. When the joint angle is between  $60^\circ$  and  $90^\circ$ , the effective stress between the holes is weakened, and the peak effective stress gradually decreases (except for  $90^\circ$ ).
3. Under the influence of the superposition of stress waves, the distribution of the peak effective stress of the rock mass element on the blasting side of the joint presents a “W” shape. With the increase of the joint angle, the stress concentration of the joint end is weakened, and the effective stress of the rock mass decreases. The peak effective stress at the three key points decreases gradually, and the blasting effect becomes worse gradually.

**Author Contributions:** Conceptualization, X.W. and X.Z.; methodology, J.Z.; software, P.Z.; validation, X.W., H.Z., and D.L.; resources, X.Z. and J.Z.; data curation, P.Z.; writing—original draft preparation, X.W.; writing—review and editing, X.Z. and H.Z. All authors have read and agreed to the published version of the manuscript.

**Funding:** This work was funded by the National Natural Science Foundation of China (No. 51874189), the Shandong Province Natural Science Foundation (No. ZR2023ME106), and the Open Fund Project of the Engineering Research Center of the Ministry of Education for Mining Underground Engineering (No. JYBGCZX2021102).

**Data Availability Statement:** Not applicable.

**Acknowledgments:** We would like to thank all the editors of this journal for their help and support in the process of publishing this paper. Thanks to all the anonymous reviewers for their constructive comments and suggestions.

**Conflicts of Interest:** The authors declare no conflict of interest.

## References

1. Cai, M.F. *Rock Mechanics and Engineering*, 2nd ed.; Science Press: Beijing, China, 2013; pp. 74–105.
2. Han, G.S.; Jing, H.W.; Jiang, Y.J.; Liu, R.C.; Su, H.J.; Wu, J.Y. The effect of joint dip angle on the mechanical behavior of infilled jointed rock masses under uniaxial and biaxial compressions. *Processes* **2018**, *6*, 49. [[CrossRef](#)]
3. Zhao, Y.; Zhao, Y.; Zhang, Z.; Wang, W.H.; Shu, J.M.; Chen, Y.; Ning, J.G.; Jiang, L.S. Investigating the influence of joint angles on rock mechanical behavior of rock mass using two-dimensional and three-dimensional numerical models. *Processes* **2023**, *11*, 1407. [[CrossRef](#)]
4. Ding, C.X.; Yang, R.S.; Chen, C.; Ma, X.M.; Kang, Y.Q.; Zhao, Y. Experimental study on the interaction between directional Crack and open joint in slit charge Blasting. *Chin. J. Eng. Sci.* **2021**, *43*, 894–902.
5. Xu, P.; Yang, R.S.; Guo, Y.; Guo, Z.C. Investigation of the blast-induced crack propagation behavior in a material containing an unfilled joint. *Appl. Sci.* **2020**, *10*, 4419. [[CrossRef](#)]
6. Li, Q.; Xu, W.L.; Wang, K.; Gao, Z.H.; Huo, S.S.; Huang, C. Study on the mechanical behavior of crack propagation effect at the end of defect under explosive load. *Int. J. Rock Mech. Mining Sci.* **2021**, *138*, 104624. [[CrossRef](#)]
7. Yang, R.S.; Xu, P.; Yang, L.Y.; Ding, C.X. Study on propagation law of explosion stress wave in jointed rock mass. *Metal Mine* **2016**, *6*, 49–54.
8. Zhang, F.P.; Peng, J.Y.; Fan, G.H.; Li, S.J.; Li, Y.H. Rock blasting mechanism of rock mass under different static stress and joint conditions. *Rock Soil Mech.* **2016**, *37*, 1839–1846+1913.

9. Liang, D.X.; Zhang, N.; Rong, H.Y. Study on crack growth test and mixed finite-discrete element numerical simulation of cross-fractured rock mass. *Rock Soil Mech.* **2023**, *44*, 1217–1229.
10. Wei, C.H.; Zhu, W.C.; Bai, Y.; Li, S. Numerical simulation of rock double-hole blasting under different joint angles and ground stresses. *Chin. J. Mech.* **2016**, *48*, 926–935.
11. Song, J.F.; Lu, C.P.; Zhang, X.F.; Guo, Y.; Yang, H.Y. Damage mechanism and wave attenuation induced by blasting in jointed rock. *Geofluids* **2022**, *2022*, 6950335. [CrossRef]
12. Fan, L.F.; Sun, H.Y. Seismic wave propagation through an in-situ stressed rock mass. *J. Appl. Geophys.* **2015**, *121*, 13–20. [CrossRef]
13. Li, X.P.; Dong, Q.; Liu, T.T.; Luo, Y.; Zhao, H.; Huang, J.H. Model test study on propagation law of explosion stress wave in jointed rock mass under different ground stresses. *Chin. J. Rock Mech. Eng.* **2016**, *35*, 2188–2196.
14. Sun, N.X.; Lei, M.F.; Zhang, Y.L.; Su, G.M.; Huang, G.F. Study on the influence of weak interlayer on the propagation process of explosion stress Wave. *J. Vibr. Shock* **2020**, *39*, 112–119+147.
15. Qu, S.J.; Liu, J.F. Study on the influence of joint angle on the effect of pre-cracking blasting. *Rock Soil Mech.* **2015**, *36*, 189–194+204.
16. Liu, W.H.; Qu, Z. Strain field evolution analysis of brittle shale with initial fractures based on DIC. *Processes* **2023**, *11*, 2319. [CrossRef]
17. Xie, B.; Li, H.B.; Wang, C.B.; Liu, Y.Q.; Xia, X.; Ma, G.W. Numerical simulation of the effect of geometric characteristics of joint on pre-cracking blasting. *Rock Soil Mech.* **2011**, *32*, 3812–3820.
18. Zhang, X.T.; Ma, L.; Yu, H.; Zhu, B.H.; Zhou, H.M.; Wang, X.Y. The empty hole diameter with confining pressure cylinder cut blasting crushing effect. *Coal Sci. Technol.* **2022**. Available online: <https://kns.cnki.net/kcms/detail/11.2402.TD.20221123.1633.008.html> (accessed on 12 August 2023).
19. Panji, M.; Habibivand, M. Seismic analysis of semi-sine shaped alluvial hills above subsurface circular cavity. *Earthq. Eng. Eng. Vib.* **2020**, *19*, 903–917. [CrossRef]
20. Panji, M.; Mojt bazadeh-Hasanlouei, S.; Fakhravar, A. Seismic response of the ground surface including underground horseshoe-shaped cavity. *Transp. Infrastr. Geotechnol.* **2021**, *9*, 338–355. [CrossRef]
21. Huang, X.Y.; Ji, Q.; Zhang, X.T.; Jiao, S.J.; Wei, H.X. Numerical simulation of rock breaking mechanism of four-hole cut blasting under earth stress. *J. Shandong Univ. Sci. Technol. (Ed. Nat. Sci.)* **2022**, *41*, 60–69.
22. Xie, L.X.; Lu, W.B.; Jiang, Q.H.; Zhang, Q.B.; Wang, G.H.; Chen, M. Damage evolution mechanism of deep rock mass during cut blasting. *J. Cent. South Univ.* **2017**, *48*, 1252–1260.
23. Dehghan Banadaki, M.M. and B. Mohanty. Numerical simulation of stress wave induced fractures in rock. *Int. J. Impact Eng.* **2012**, *40*, 16–25. [CrossRef]
24. Zhang, X.T.; Dong, G.Q.; Yu, H.; Zhang, J.S.; Zhou, H.M.; Zhu, B.H.; Yin, Z. Effect of empty hole diameter on vibration of straight Cut blasting under confining pressure. *J. Shandong Univ. Sci. Technol. (Ed. Nat. Sci.)* **2023**, *42*, 44–52.
25. Shao, Z.S.; Gao, J.P. Simulation analysis of blasting damage characteristics of slit charge. *Eng. Blasting* **2020**, *26*, 35–41.
26. Zhang, X.T.; Li, J.; Li, D.; Xie, S.Z.; Zhou, H.M.; Li, T.C. Numerical simulation of parallel cutting with different number of empty holes. *Teh. Vjesn.* **2021**, *28*, 1742–1748.
27. Wang, Y.B.; Lei, Q.; Yang, R.S.; Xu, P. Numerical analysis of Crack growth in defective media under explosion load. *Blasting* **2017**, *34*, 1–6+24.
28. Cho, S.H.; Nakamura, B.Y. Mohanty Numerical study of fracture plane control in laboratory-scale blasting. *Eng. Fract. Mech.* **2008**, *75*, 3966–3984. [CrossRef]
29. Li, X.F.; Li, H.B.; Liu, K.; Zhang, Q.B.; Zou, F.; Huang, L.X. Study on dynamic and fracture characteristics of rock under impact loads. *Chin. J. Rock Mech. Eng.* **2017**, *36*, 2393–2405.
30. Yang, X.L. *Damage Mechanism of Rock Blasting and Its Effect on Surrounding Rock*; Science Press: Beijing, China, 2015; pp. 20–22.

**Disclaimer/Publisher’s Note:** The statements, opinions and data contained in all publications are solely those of the individual author(s) and contributor(s) and not of MDPI and/or the editor(s). MDPI and/or the editor(s) disclaim responsibility for any injury to people or property resulting from any ideas, methods, instructions or products referred to in the content.